FRET-Mediated Collective Blinking of Self-Assembled Stacks of CdSe Semiconducting Nanoplatelets

Zakarya Ouzit, Jiawen Liu, Juan Pintor, Benoît Wagnon, Lilian Guillemeney, Benjamin Abécassis, Laurent Coolen

FRET-mediated Collective Blinking of Self-Assembled Stacks of CdSe Semiconducting Nanoplatelets

Zakarya Ouzit[1], Jiawen Liu[1], Juan Pintor[1], Benoît Wagnon[2], Lilian Guillemeney[2], Benjamin Abécassis[2] and Laurent Coolen[1*]

1. Sorbonne Université, CNRS, Institut des NanoSciences de Paris, INSP, F-75005 Paris, France
2. ENSL, CNRS, Laboratoire de Chimie UMR 5182, 46 allée d'Italie, 69364 Lyon France
*Email : laurent.coolen@sorbonne-universite.fr

Abstract

Förster resonant energy transfer (FRET) can be an efficient energy transfer mechanism between densely-packed fluorescent emitters. It plays a key role in photosynthesis but may also be detrimental. In opto-electronic devices for instance, FRET funnels energy to quenching sites and favours losses. Here, we image individual self-assembled chains of stacked CdSe nanoplatelets and demonstrate fluorescence intermittency (blinking) of chain portions corresponding to a few tens of platelets. This collective blinking is attributed to the fluctuations of a quencher site, to which excitons are transferred by FRET migration from the surrounding platelets. We develop an analytical random walk model of the chain and show that an ensemble of platelets can be quenched collectively by a single site provided that its quenching (non-radiative recombination) rate is faster than the geometric mean of the radiative recombination rate and the transfer rate, which for self-assembled platelets would be of the order of $(100\ \mathrm{ps})^{-1}$.

Keywords : semiconductor nanoplatelets ; Förster transfer ; fluorescence blinking

Since its first implementations,[1,2] single-molecule spectroscopy has revealed many photophysical properties inaccessible to ensemble measurements. A prominent example is fluorescence on/off intermittency (blinking), which was evidenced on a wide range of emitters such as terrylene molecules,[3] colloidal semiconductor nanocrystals[4] or fluorescent proteins.[5] These studies use very dilute depositions of fluorophores (less than $1/\mu m^2$) so that the luminescence of single emitters can be isolated. However, most applications of these fluorophores involve densely-packed samples where close-range interactions can modify luminescence significantly. For instance, a large collection of blinking emitters should not blink because their blinking events are averaged out. Yet, various types of fluorophore assemblies, when considered individually, have demonstrated on/off blinking, showing that all fluorophores within the assembly fluctuate collectively. Such collective blinking was reported for some multichromophoric dendrimers[6] and conjugate polymers,[7-10] aggregates of polymer chains,[11] J-aggregates,[12,13] dye-loaded nanospheres[14] and clusters of semiconductor nanocrystals.[15,16]

Occurrences of collective blinking have been explained by various mechanisms involving (i) a quencher site whose non-radiative decay mechanism switches on and off randomly, and (ii) Förster resonant energy transfer (FRET), a non-radiative dipole-dipole interaction ranging over a few nanometres, by which an exciton in a given fluorophore recombines and yields its energy to a neighbour fluorophore.[17] The quencher whose on/off fluctuations are responsible for blinking may act on a collection of emitters through direct (one-jump) FRET[8] or most often by exciton diffusion until it reaches the quencher.[9-14,18] For clusters of nanocrystals, due to their inhomogeneous distribution of

energies, observations show that the exciton can be funnelled to the lowest-energy nanocrystal, and blinking is controlled by the fluctuations of this acceptor.[15,16] These mechanisms must be understood in order to mitigate the effect of quencher states on the luminescence of a dense sample. Moreover, collective blinking provides crucial insights into exciton transfer processes, by which energy is funnelled in photosynthesis systems[19] and which have been proposed for opto-electronic applications.[20]

Whereas collective blinking has been observed for collections of up to hundreds of dye molecules,[12,14] for semiconductor nanocrystals it was limited to trimers[15] and small clusters,[16] (and modifications of on-time statistics were also observed for clusters of tens of nanorods[54]) because their interparticle distances are larger so that FRET is less efficient. Semiconductor nanoplatelets[21] (NPL) present exceptional photophysical properties with various potential opto-electronic applications.[22-24] They also display very fast FRET transfer[20,25-27] due to their low Stokes shift, negligible inhomogeneous linewidth[28] and large oscillator strength.[21] Moreover, when stacked co-facially, their in-plane dipoles[29] have deterministic parallel orientation.[30] Demir et al. proposed that FRET exciton diffusion is responsible for the lower quantum yield of stacked NPLs by transferring excitons to quencher platelets.[25]

Self-assembled chains of stacked nanoplatelets[31-35,55] constitute excellent model systems to study charge transfer and interactions between nano-emitters. The NPLs can be arranged in linear order over up to a few microns, with a uniform centre-to-centre distance around 5 nm. While reported exciton diffusion lengths were limited to 5-30 nm in films[36] or ordered lattices[37,38] of spherical nanocrystals, we have shown that excitons diffuse along a NPL chain over an exceptional length of 500 nm before recombining.[39]

In this paper, we demonstrate collective blinking of large 400-nm portions of self-assembled chains corresponding to a few tens (35-70) of nanoplatelets. We attribute this observation to FRET migration of excitons to fluctuating quencher platelets. We develop an analytical model of random walk diffusion in presence of a defect site and discuss the quenching range and rate.

Results and discussion

We synthesized nanoplatelets with a 1.5-nm thickness (6 Cd layers + 5 Se layers), with $(7 \pm 2) \times (20 \pm 4)$ nm² lateral dimensions (TEM image in figure 1(a)) (see Methods). The emission spectrum of the platelets is centered at 549 nm (figure 1(b)). No inhomogeneous broadening is observed when comparing the emission spectra of single NPL and NPL chains, because of the monodisperse NPL thickness controlled with atomic layer precision. The assembly took place through slow evaporation of a nanoplatelet dispersion in the presence of oleic acid. 1D chains of platelets were obtained as shown on the TEM image of figure 1(c). The center-to-center distance between neighbor platelets is homogeneous and estimated as 5.7 nm from TEM images. The lengths of the chains obtained range from a few hundreds of nm to a few µm for the longest observed.[40]

We show on figure 1(d) the fluorescence image of a 2 µm single chain obtained with our micro-photoluminescence setup, under wide-field excitation at 450 nm at sufficiently low power density that no more than one exciton per chain was created (see Supporting Information – S.I. – section E). In order to study the fluctuations of the intensity along the axis of the chain, we deconvolved the images

by the point spread function (PSF) of the imaging setup (see S.I. section A ; PSF radius 190 nm). The deconvolved version of the image on figure 1(d) is shown in figure 1(e): the width of the chain has decreased and some bright or dark portions appear more clearly.

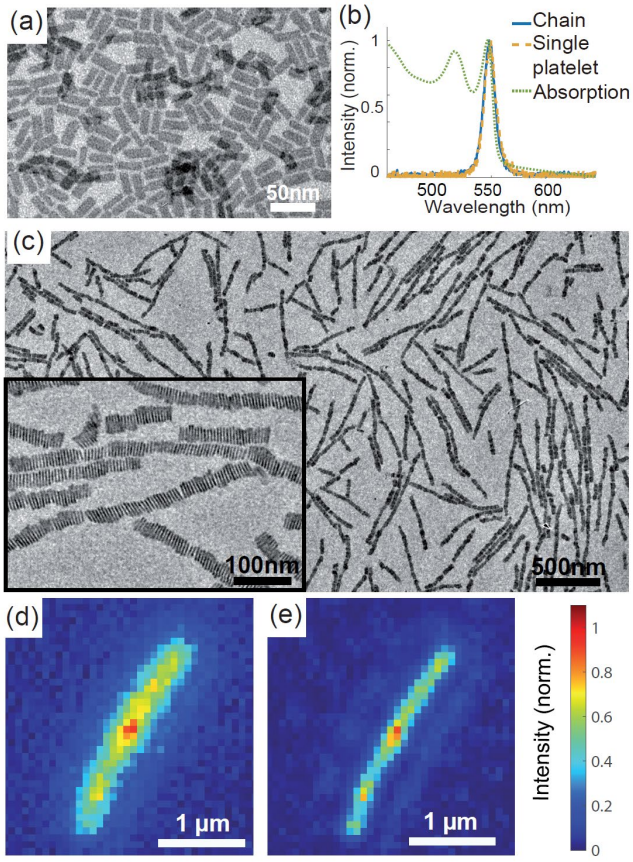

Figure 1. (a) TEM image of single CdSe nanoplatelets. (b) Absorption spectrum (green dotted line) of a NPL solution. Photoluminescence spectra of a single NPL (yellow dashed line) and a NPL chain (blue full line) under 470 nm excitation. (c) TEM image of NPL chains. (d) Fluorescence image of a NPL chain under wide-field excitation at 450 nm. (e) Same image with the imaging system PSF deconvolved. Same colorbar for both figures (d) and (e).

Figure 2(a) shows the deconvolved fluorescence images of the same chain at different times (similar figures for other chains are plotted in the S.I. file and the original video files are available online as supporting material). The intensity is not homogeneous along the chain. Some portions display fluorescence intensity fluctuations. We plot in figure 2(b) the time-position fluorescence diagram of the chain, giving its fluorescence profile as a function of time. We can identify *on* states of emission (red rectangles) and *off* (fully dark) states of emission (black rectangle). We plot on figure 2(c) the intensity of three points of the chain as a function of time. The intensity-time curves of remotes points present no clear correlation with each other, showing that each portion blinks independently from the others.

This is confirmed by plotting (fig. 3(a)) the two-dimensional autocorrelation function $C(x,\tau)$ of this time-position diagram, revealing correlations in both time and space coordinates. When plotting $C(x,\tau)$ as a function of x (fig. 3(b)), for $\tau = 0$ correlations appear over a distance of the order of 200 ± 100 nm (distance for $1/e$ decay of $1 - C$). These correlations are maintained for delays of 0.2 or 0.5 s, but are mostly lost for τ = 10 s as most blinking events are shorter. Equivalently, when plotting

$C(x,\tau)$ as a function of τ (fig. 3(c)), for $x = 0$ (time correlations of a given point) strong correlations are observed at short delays, indicating the presence of blinking over 0.1-to-1 s time scales. These correlations are maintained for x up to 200 nm. On the other hand, for points separated by x = 400 nm or more (fig. 3(c)), signs of blinking vanish. This confirms that different portions of the chain present uncorrelated blinking. Eventually, the autocorrelation plots show that a given spot on the chain will blink in synchronized manner with neighbor points $\pm$ 200 nm from it : this corresponds to portions of the chain of length 400 ± 200 nm (70 NPLs) blinking together.

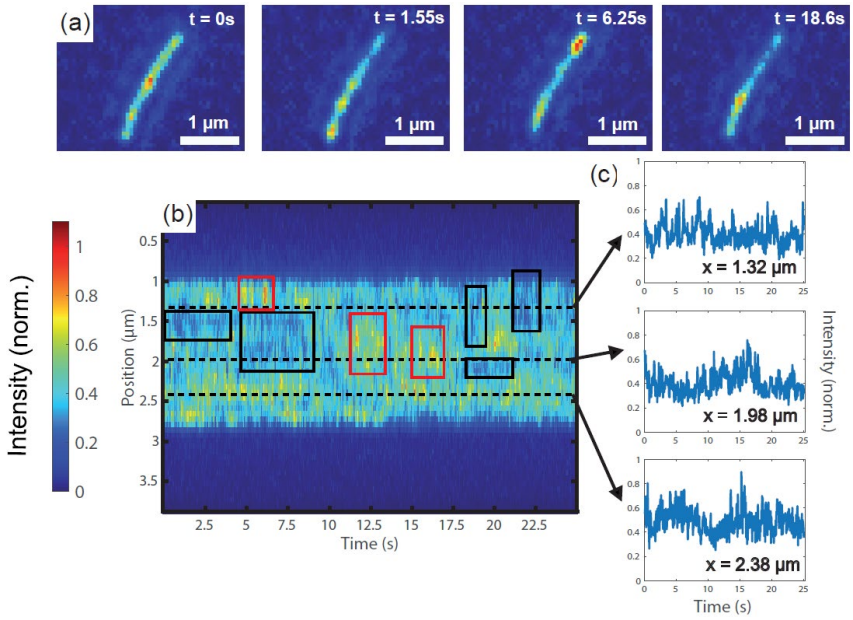

Figure 2. (a) Deconvolved fluorescence images of a nanoplatelets chain (same as in figure 1(d)) under wide-field excitation at 450 nm taken at different times. (b) Time-position diagram showing the intensity along the chain (vertical) versus time (horizontal), showing collective blinking with bright spots (red rectangles) and dark spots (black rectangles). (c) Intensity of three points of the chain (black dashed line on figure 2(b)) versus time. Same colorbar for figure 2(a,b). Examples of such treatment for other chains are provided in section B of the S.I.

A fluorescence spot on the camera corresponds to many platelets, and the blinking of each single platelet cannot be resolved individually as the NPL-to-NPL distance (5.7 nm) is much lower than the PSF (190 nm) – even when deconvolving the PSF. However, precisely because the luminescence from a spot on the chain is the sum of many platelets, if these platelets blinked randomly out-of-phase from each other, their blinking would be averaged out in the summation and no significant intensity fluctuation would be observed on the chain. The fact that portions of the chain blink and can become randomly extinct (fig. 2(b)) indicates that many NPLs within this portion fluctuate in phase, correlated with each other.

More precisely, if the signal is a sum of N emissions, uncorrelated but of same statistical properties (same average intensity and intensity correlations for each single emitter), the correlations scale as $1/N$:

$$C(\tau) - 1 = \frac{C_0(\tau) - 1}{N}$$

where $C_0(\tau)$ is the correlation function of a single emitter (demonstration in S.I. section F). We measure here, on average, the autocorrelation $C(x = 0, \tau = 0) = 1.09$ for the chains and $C_0(\tau = 0) = 1.35$ for isolated platelets on a glass slide (see fig. S8). If all nanoplatelets within a chain portion of the size of the PSF ($N \sim 35$) blinked independently, there would be almost no blinking in the total intensity and this would be reflected in the intensity correlation: $C(0) - 1 = (C_0(0) - 1)/N = 0.01$, while the measured correlations are almost one order of magnitude larger: $C(0) - 1 = 0.09$. This confirms that a large number of platelets blink collectively. However, the chain correlations (1.09) are still not as large as the single-NPL correlations (1.35). This is probably due to the averaging over the whole chain, which contains both blinking and non-blinking portions, and possibly also because the blinking statistics are different for isolated NPLs and platelets in a chain. Yet we cannot exclude that only a portion of the chains in a given spot blink collectively. In the latter case, a detailed analysis of the correlations (see S.I. section F) shows that around half of the emitters would blink in phase.

Eventually, with intensity correlations spanning around 400-nm portions (70-NPL) of the chains and correlation amplitudes revealing that at least half of the emitters fluctuate in phase, we conclude that a few tens of NPLs (35 to 70) blink collectively. This should not happen if the blinking of each platelet was controlled by a specific quencher defect fluctuating randomly, independently from the others, because each quencher defect has its own random fluctuations. Therefore, we conclude that the blinking of many platelets in a given portion is controlled collectively by the same single quencher.

In order to understand this mechanism, let us first discuss the blinking of isolated NPLs. Figure 4(a) shows the fluorescence intensity of a single nanoplatelet (identified as single by its antibunched behavior) as a function of time. It shows clear switches between *on* (bright) and *off* (dark) periods. Blinking studies often distinguish “type A” and “type B” behaviors:[41] in the former, periods of lower light emission are associated with faster exciton recombination, indicating the appearance of an additional non-radiative decay channel. In the latter, the decay curve remains unchanged, showing that the quenching mechanism involves bypassing the emitter state (figure 4(b)). A widespread “type A” blinking mechanism for semiconductor nanoparticles is ionization/neutralization of the particle: during charged periods, an additional non-radiative decay channel for the exciton is introduced by its Coulombic interaction with the extra charge (Auger effect).

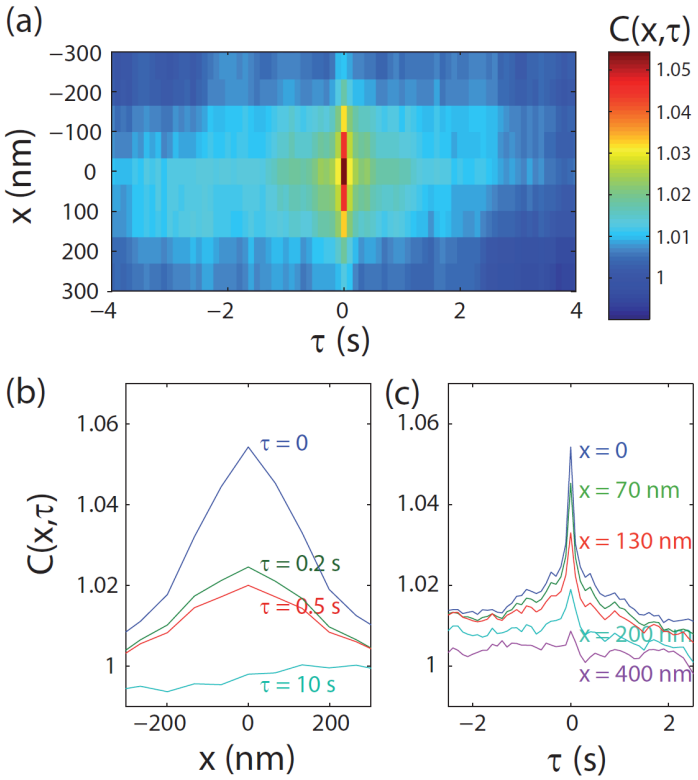

Figure 3. (a) 2-dimensional autocorrelation function $C(x,\tau)$ of the time-position diagram of fig. 2(b). (b) Spatial dependence of the correlations at various delays τ. (c) Time dependence of the correlations for various distances x.

Figure 4(c) plots the decay curve of brighter and dimmer periods of the NPL in figure 4(a). Both curves present a main short component and a minor long component. The short component is 7.1 ns for the brighter states and 1.8 ns for the dimmer states, showing that the dimmer states are associated with much faster decay. The slow component, on the other hand, is longer for the dimmer states (128 ns) than for the brighter states (58 ns). More decay curves are presented in S.I. section C. Figure 4(d) shows, for the same recording, the fluorescence-lifetime-intensity-distribution (FLID) giving the correspondence between the fluorescence intensity and the decay time at each moment of the blinking curve. Both curves show that the luminescence decay is faster when the emitter is less bright, corresponding to a type A blinking for our nanoplatelets.

More information can be obtained from the literature on similar platelets. At 4 K, spectral fluctuations have been attributed to a switching between exciton and trion luminescence, corresponding to either neutral or negatively charged NPL states.[42-44] At room temperature, NPL blinking can be understood as a dimming of the negatively charged NPL luminescence due to non-radiative Auger recombination of the trion. However, Weiss et al. have distinguished blinking slower than 1 s., attributed to trion states and correlated with spectral shifts, and sub-second blinking demonstrating type-B behavior.[45] In one instance, different emissive states were also evidenced, associated with either exciton or trap states.[46] The more general literature on semiconductor nanoparticle blinking has shown that it depends on many parameters like nanoparticle ligand coating or protective shell (here blinking is probably favored by the absence of protective shell on the NPLs)

and that higher excitation photon energy and power density can enhance blinking by reducing the average duration of the *on* periods.

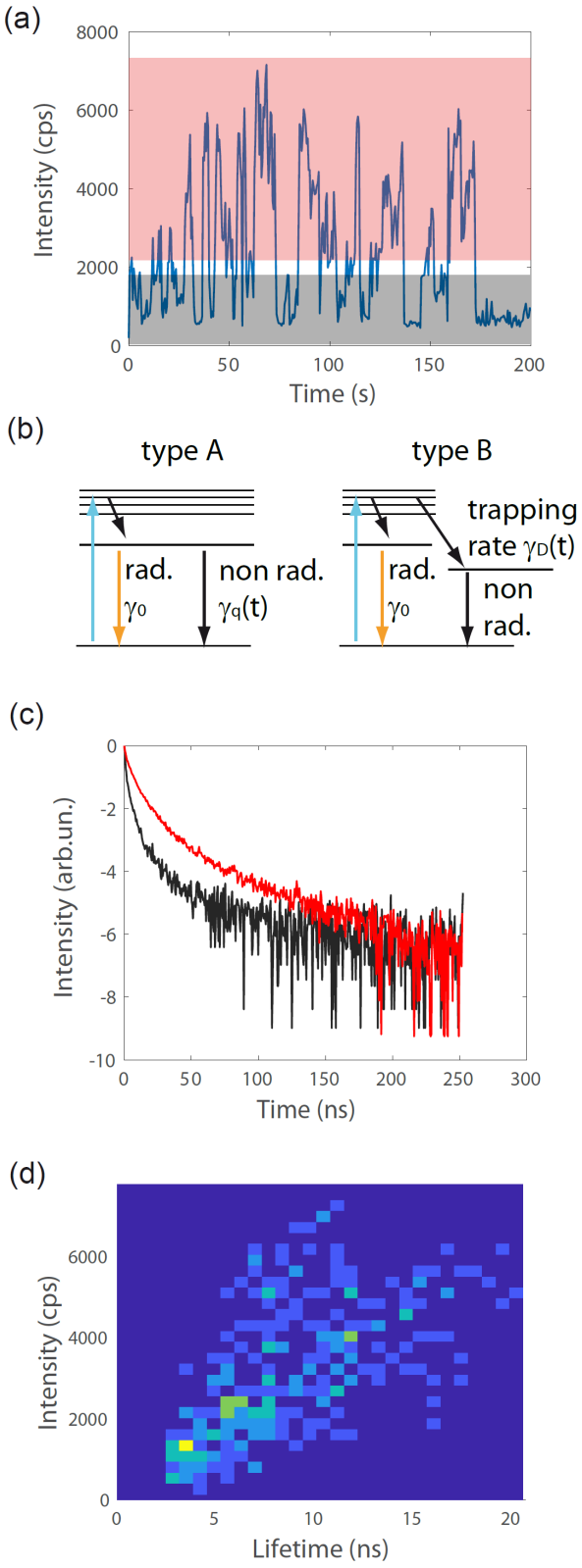

Figure 4. Blinking of a single nanoplatelet. (a) Intensity time trace (time bin = 0.5 s). (b) Schematic of type-A and type-B blinking behaviors. (c) Decay curves (semilog scale) of *on* states (red) and *off* states (black) of emission from the fluorescence data of figure 3(a) (red and black rectangles). (d) Fluorescence lifetime-intensity

distribution extracted from the fluorescence data of figure 3(a). Examples of such treatment for other single platelets are provided in section S.I.-C.

Based on this analysis of single-NPL blinking, we propose the following mechanism for collective blinking. A given nanoplatelet blinks back and forth from off to on states because of the appearance and disappearance of a new non-radiative decay channel (Auger or other) which bypasses radiative emission (type-A blinking). When this platelet is off, excitons from nearby platelets can be transferred to this platelet and decay non-radiatively by the same mechanism. If transfer to the off-platelet and non-radiative decay is faster than photon emission, the off-platelet will act as a quencher for its whole neighbors group.

More precisely, efficient transfer from a platelet to the neighbor platelet can occur by FRET, as is well known for stacked platelets.[20,25-27,39] Collective blinking from a 400-nm chain portions is achieved if excitons can transfer to a single quencher from all of these platelets. The range of FRET transfer (Förster radius) is theoretically of the order of 17 nm for NPLs:[39] this is especially large but much shorter than 400 nm. Therefore, we exclude that all NPLs transfer their excitons directly to the quencher. Eventually, we propose that excitons transfer to the quencher by FRET diffusion: neighbor-to-neighbor FRET hopping. Such FRET diffusion to a quencher, shown in figure 5(a), has already been described in order to explain the low quantum yield of stacked NPLs.[25] This mechanism, combined with on/off fluctuations of the quenching channel, explains the observed collective blinking. Note that the blinking - fluctuations of the quencher efficiency – occurs on time scales (seconds) much longer than the quenching of a single excitation (ps, ns). The efficiency of this FRET-mediated quenching mechanism will result from a competition between non-radiative decay at the quencher site and radiative decay in all platelets, and also, at the quenching site, a competition between escape from the site by FRET and non-radiative decay.

In order to find the figure of merit which determines this competition, we consider an ordered infinite one-dimensional (1D) array of identical nanoplatelets, with a homogeneous centre-to-centre distance between neighbour platelets, so that all platelets present the same rates of radiative recombination γ_0 and of FRET transfer to a neighbour platelet γ_{tr} (fig. 5(a)). Because FRET scales as the 6th power of distance, we limit our model to nearest-neighbour jumps: second-neighbour jumps might occur but with negligible influence. The radiative decay rate is obtained from on-state decay curves and is of the order of (0.1 ns)$^{-1}$.[39,47] We estimated the transfer rate as $\gamma_{tr}\sim$ (1 ps)$^{-1}$.[39] Each NPL being labelled by its index s (integer number from $-\infty$ to $+\infty$), a quencher NPL is introduced at site $s = s_q$, with an additional non-radiative rate γ_q. We measure experimentally the distribution of luminescence intensity over the NPL chain which is given by the probability that an exciton recombines at NPL s and emits a photon. We model this system as a 1D-random walk of the exciton with jumps separated by $1/\gamma_{tr}$.[48] The full analytical treatment for this problem is developed in section D of the S.I. When all excitons are created at the same nanoplatelet $s = s_0$ (localized excitation), the luminescence distribution can be written

$$I_{s_0}(s) \propto e^{-|s-s_0|/s_F} - Qe^{-|s_q-s_0|/s_F}e^{-|s-s_q|/s_F} \qquad (1)$$

with the two figures of merit Q and s_F defined in the S.I. The factor Q depends on γ_{tr}, γ_0 and γ_q and therefore reflects the influence of quenching (with $Q \to 0$ for $\gamma_q \to 0$ and $Q \to 1$ when $\gamma_q \to \infty$), while s_F depends only on γ_{tr} and γ_0 and characterizes the FRET efficiency.

We plot in figure 5(b) this function $I_{s_0}(s)$ giving the intensity along the chain under localized excitation at position $s_0 = -100$ with a single quencher localized at $s_q = 0$ for different values of Q. For $\gamma_{tr} = 10^{12}$ s^{-1} and $\gamma_0 = 10^8$ s^{-1}, $s_F = 100$. For $Q = 0$ (absence of quenching), the curve simply reflects the exciton diffusion, starting from the excitation position s_0, with a diffusion range s_F. When Q increases, a luminescence drop appears at the quencher position $s = s_q$. When Q tends to 1, the quenching is so strong that the exciton can never go beyond the quenching site: $I(s \geq s_q) = 0$.

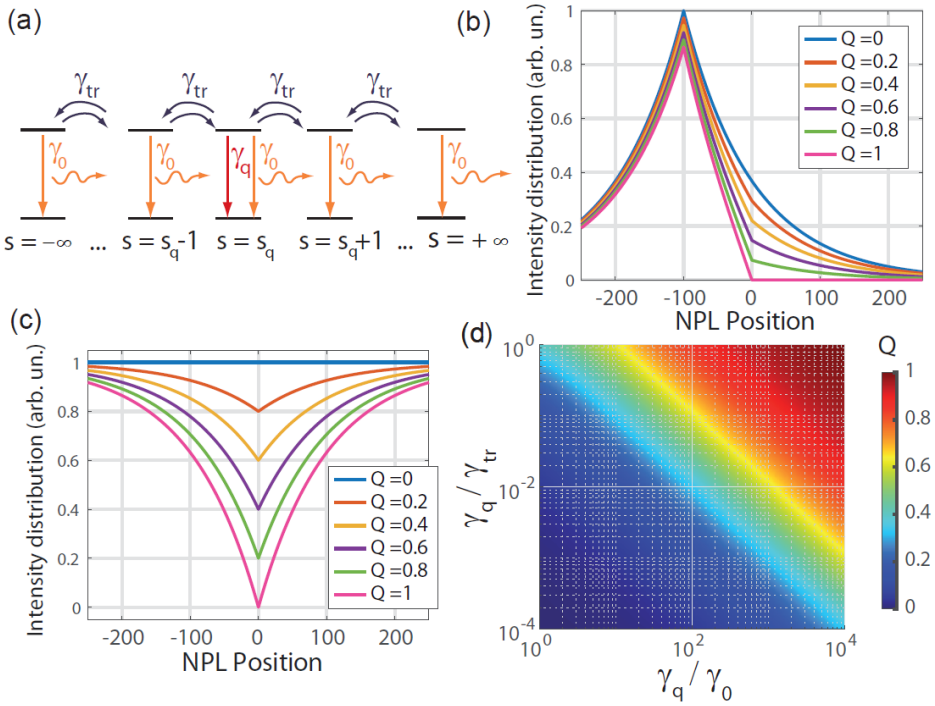

Figure 5. (a) Model for collective blinking : each NPL is a two-level system labeled by its integer position s with decay rate γ_0 and transfer rate to its neighbors γ_{tr}. The quencher NPL is described as an additional decay rate γ_q for one NPL numbered s_q. (b) Intensity distribution along a NPL chain under localized excitation calculated with the random walk model for different values of the quenching factor Q with s_F = 100. A single exciton is generated at position $s_0 = -100$ in the presence of a single quencher at $s_q = 0$. (c) Intensity distribution along a NPL chain under uniform excitation calculated with the random walk model for different values of the quenching factor. A single quencher is considered at position $s_q = 0$. (d) Evolution of the quenching factor Q with the two ratios γ_q/γ_{tr} and γ_q/γ_0.

In order to match the experimental conditions, which are chains under a uniform wide-field excitation, we summed the distribution $I_{s_0}(s)$ over all possible values of s_0, which leads to (see S.I.)

$$I(s) \propto 1 - Qe^{-|s-s_q|/s_F} \qquad (2)$$

Figure 5(c) shows this emission profile $I(s)$ for different values of Q for the same values of γ_{tr} and γ_0. The emission intensity is uniform ($I(s) = 1$) in the absence of quenching. As soon as $Q \neq 0$, the intensity drops at the centre of the chain, with no intensity at $s = s_q$ for $Q = 1$. We can conclude that the observation of collective quenching (dip in the luminescence profile) is well described by our

model. The quenching efficiency (depth of the luminescence dip) corresponds to factor Q, while coefficient s_F describes the quenching range.

We show on figure 5(d) the dependence of Q on the two ratios γ_q/γ_0 and γ_q/γ_{tr}. Domains of weak ($Q \ll 1$) and efficient ($Q \sim 1$) collective quenching can be distinguished. Collective quenching requires FRET transfer to be much faster than recombination ($\gamma_{tr} \gg \gamma_0$), so that the excitons diffuse before recombining. In this case, we can approximate our two parameters as

$$s_F = \sqrt{\frac{\gamma_{tr}}{\gamma_0}} \quad \text{and} \quad Q = \frac{1}{1+2\frac{\sqrt{\gamma_0\gamma_{tr}}}{\gamma_q}} \qquad (3)$$

An experimental value of the blinking portion size of $2s_F$ = 70 NPLs (400 nm) was extracted from figure 3, with a significant uncertainty given the pixel size and noise ratio. This value of 200 nm is shorter than the FRET diffusion length of 500 nm which we reported previously,[39] either because of these uncertainties, or as a result of a slightly different sample preparation, or because of the limitations of the theoretical model. For instance, structural disorder within the chain (fig. 1(c)) might prevent exciton transfer at some locations and reduce the overall average diffusion length.

From eq. (3) the condition for efficient quenching ($Q \to 1$) writes simply

$$\gamma_q \gg \sqrt{\gamma_0\gamma_{tr}} \qquad (4)$$

Let us provide a physical intuition for this condition: because the exciton diffuses on average over s_F platelets, it will be at the quencher NPL at a given time with a probability of the order of $1/s_F$ (provided that it was created at a distance smaller than s_F from the quencher). Therefore, one can consider γ_q/s_F as the time-averaged quenching rate: it must be faster than γ_0 in order to obtain collective quenching, which leads to equation 4.

With the measured single-NPL exciton decay time of $1/\gamma_0 \sim 10$ ns and our previous estimate[39] of $1/\gamma_{tr}$ in the order of 1 ps, condition (4) means that the quenching time scale must be faster than 100 ps. Alternatively, we may use the experimental value $s_F \sim 35$ and write the quenching condition $\gamma_q/s_F \gg \gamma_0$: then the quenching must be faster than 300 ps. If the blinking is attributed to a charged NPL and Auger recombination, the quenching rate corresponds to the trion Auger rate which is known to be slower than 1 ns at 5 K,[43] but should be faster at room temperature. More experimental information is available about the *biexciton* Auger rate (which may be of the order of twice the *trion* Auger rate[42]). By transient absorption or time-resolved photoluminescence measurements, values of the biexciton Auger rate ranging from 70 to 600 ps have been reported for 4-monolayer NPLs at room temperature, [22,49-51] depending mostly on the NPL lateral area. However, Auger times of 2-3 ns have also been deduced from time-gated antibunching data,[52] while on the other hand Auger-mediated hole trapping mechanisms can also occur on sub-picosecond timescales.[53] A quenching rate $1/\gamma_q \sim 35$ ps has been used to model stacked NPLs.[25]

Eventually, it seems plausible that condition (4) can be fulfilled for some NPLs, with a non-radiative rate γ_q related to Auger effect or to another mechanism. Although most single NPLs exhibited some level of blinking, we note that a relatively small portion of NPLs behave as quenchers in the chains: around 5-10 blinking domains appear in a chain of 350 NPLs, corresponding to 1-3 % of quenchers. This might be a sign that the quenching condition (4) is not easily fulfilled, because Auger effect is not very

fast in platelets, so that not all defective platelets can act as collective quenchers. This might also be due to a better ligand coverage and surface passivation within the chain than on single platelets. Indeed, the number of blinking sites in a chain depends on the assembly protocol and sample deposition. For the samples presented in figure 2 and S.I.-C, all chains showed some level of blinking. On the other hand, other samples showed no blinking for 90 % of the NPL chains, probably due to better NPL surface passivation or because the stacking structure was better preserved during spin coating. When the same chain solution was sonicated for 20 minutes before deposition, the percentage of non-blinking chains was reduced to 10 % depending on the sample, reflecting some degradation of the NPL ligand coverage. This might also explain why we find around 1-3 % of platelets behaving as quenchers in our chains while Guzelturk et al. found 20 % of quenchers for their more disordered stacks of platelets.[25]

To conclude, we have used linear self-assembled NPL chains to analyze the effect of FRET on the luminescence properties of an ensemble of nano-emitters. We evidenced events of collective luminescence intermittency over some portions of chains involving an exceptional collection of tens of NPLs. We attribute this observation to the presence of intermittent quencher NPLs presenting an additional non-radiative exciton decay mechanism, such as Auger trion recombination. An exciton in a given NPL may reach the quencher NPL by FRET hopping between neighbor platelets if the FRET and quenching rates are sufficiently large. We developed an analytical random walk model to describe this effect and showed that the collective quenching should involve around $s_F \sim \sqrt{\gamma_{tr}/\gamma_0}$ platelets and be efficient under the condition $\gamma_q \gg \sqrt{\gamma_0 \gamma_{tr}} \sim$ 1/(100 ps). Collective blinking of single NPL chains thus provides new direct insight into the physics of FRET-mediated quenching within dense ensemble of nano-emitters. In order to reduce FRET-mediated quenching, the different strategies include reducing the number of defective NPLs (low γ_q), accelerating radiative decay (high γ_0) so that the exciton recombines before reaching the quencher, and, somehow less intuitively, accelerating FRET transfer (high γ_{tr}) in order to compete with non-radiative decay.

Methods

- Reagents

Sodium oleate (82%), ethanol, methanol (99%), selenium powder (99.5%), cadmium acetate dihydrate (98%) and oleic acid (90%) were purchased from Sigma-Aldrich. 1-octadecene (ODE, 90%) and hexane (90%), were supplied by Fisher-Acros Organics. Ethyl acetate (99%) and cadmium nitrate tetrahydrate (98.5%) were supplied by Fisher-Alfa Aesar. Polyisobytylene succinimide (PIBSI, mean Mw= 1000 g/mol) was a gift from TotalEnergies Additives & Fuels Solutions and was received as a 50% wt dispersion in C10 aromatic solvent. All chemicals were used without further purifications.

- Cadmium oleate synthesis

In a 1L three neck round bottom flask, 12.1776 g of sodium oleate are dissolved in 200 mL ethanol at 96° at 70°C in the presence of 5 mL of water. In parallel, 6.1996 g of cadmium nitrate tetrahydrate are dissolved in 50 mL ethanol at 96° in a conical flask. The cadmium nitrate tetrahydrate solution is then added drop by drop during 30 min. The mixture is left to react during 2 h. Purification of the obtained

precipitate is carried out by centrifuging 5 min at 6000 rpm four times in 30 mL of warm ethanol and once in 30 mL of methanol. Finally, the solid is filtered and freeze-dried overnight.

- NPL synthesis

808 mg of cadmium oleate, 27 mg of selenium powder and 25 mL ODE are inserted in a 50 mL three-neck round bottom flask. This mixture is degassed under vacuum for 1 h. The temperature is then raised to 240°C under argon flow. At 205°C, when the color is yellow-orange, 280 mg of cadmium acetate dihydrate are swiftly injected. The mixture's color shifted from yellow-orange to deep red. Annealing at 240°C is carried out during 10 min before injecting 1 mL of oleic acid and cooling down the flask to room temperature using a water bath.

NPLs are separated from the remaining reactants and quantum dots by centrifuging the crude product during 10 min at 6000 rpm. Further purification by selective precipitation and centrifugation at 6000 rpm (10 min) are carried out in presence of 10 mL ethyl acetate to remove the remaining quantum dots. After each centrifugation, NPLs are re-dispersed in first 5 mL then 2.5mL hexane.

- Chain synthesis

172 µL of the previously prepared NPL solution are mixed with hexane and a volume of oleic acid between 13 and 38 µL (corresponding to concentrations in the final dispersion of 11 to 30 mM). Hexane and NPL solution quantities are adjusted so that the total volume of the solution is to 4 mL with an absorbance of 3.6 at 550 nm. The solvent is then left to evaporate over three days and the chains are then dispersed in hexane for further use.

- TEM imaging

TEM images were taken with a JEOL JEM-1400 equipped with a 100-kV field emission gun at CIQLE, Lyon. 100 µL of 0.38% w/w PIBSI solution is added to the diluted chain solution before drop casting (1 drop) on a copper/carbon 300 mesh TEM grids. PIBSI acts as a dispersant that prevents chain aggregation and allows a better observation.

- Fluorescence microscopy

We performed optical measurements using a home-built inverted fluorescence microscope. To image the NPL chains, we used a mercury lamp for wide-field excitation (filtered by a 480-nm longpass filter which selected the 436-nm mercury line) and a CCD camera (QImaging Retiga EXi, pixel size 6.45µm corresponding to 66 nm on the image) for detection. We used an immersion objective (Olympus apochromat 100x, 1.4 N.A.) to both excite the emitters and collect their emission. The excitation power density was estimated to 5 µW/µm² (see S.I. section E). The scattered excitation light was filtered by a set of filters, and only the 549 nm fluorescence can reach the detectors. We acquired fluorescence movies of chains of nanoplatelets at around 10 frames per second. The decay curves (fig. 4) were obtained with avalanche photodiodes of resolution 200 ps. The short component decay time was estimated as the time for $1/e$ decay. The long component decay time was found by fitting the $t > 100$ ns portion of the curve by an exponential.

From the time-position diagram $I(X,t)$ (fig. 2(b)), the autocorrelation function was calculated as

$$C(x,\tau) = \frac{\langle I(X,t)I(X+x,t+\tau)\rangle}{\langle I(X,t)\rangle\langle I(X+x,t+\tau)\rangle}$$

The samples were carefully prepared in order to maintain the integrity of the chains once deposited. The glass slide was first rinsed with hexane. Then, the solution of chains was spin-coated along with pure hexane in order to dilute smoothly the solution at 4000 rpm for 40 s. The samples then presented droplets on the glass surface where preserved chains were imprisoned. The glass slide was put in vacuum in order to evaporate the droplets.

Associated contents

Supporting Information. (A) Image processing (B) Collective blinking of other chains (C) Blinking behavior of single nanoplatelets (D) Random walk model (E) Excitation regime (F) Chain and single-emitter correlation functions.

Chains blinking videos. AVI files organized by the number of the figure where the images are referenced in the main text and the supporting information.

Acknowledgements

We thank Frédéric Tort from TotalEnergies Additives & Fuels Solutions for the gift of the PIBSI polymer sample.

Funding sources

The present work was funded by the French Agence Nationale de la Recherche (project Foenics ANR-20-CE30-0012). This article is part of a project that has received funding from the European Research Council (ERC) under the European Union's Horizon 2020 research and innovation programme (Grant agreement No. 865995).

References

[1] W. E. Moerner and L. Kador, Optical detection and spectroscopy of single molecules in a solid, Phys. Rev. Lett. 62, 2535 (1989),

[2] M. Orrit and J. Bernard, Single pentacene molecules detected by fluorescence excitation in a p-terphenyl crystal, Phys. Rev. Lett. 65, 2716 (1990),

[3] Th. Basché, S. Kummer and C. Bräuchle, Direct spectroscopic observation of quantum jumps of a single molecule, Nature 373, 132 (1995),

[4] M. Nirmal, B. O. Dabbousi, M. G. Bawendi, J. J. Macklin, J. K. Trautman, T. D. Harris and L. E. Brus, Fluorescence intermittency in single cadmium selenide nanocrystals, Nature 383, 802 (1996),

[5] R. M. Dickson, A. B. Cubitt, R. Y. Tsien and W. E. Moerner, On/off blinking and switching behavior of single molecules of green fluorescent protein, Nature 388, 355 (1997),

[6] F. C. de Schryver, T. Vosch, M. Cotlet, M. van der Auweraer, K. Müllen and J. Hofkens, Energy dissipation in multichromophoric single dendrimers, Acc. Chem. Res. 38, 514 (2005),

[7] Kristin S. Grussmayer, Florian Steiner, John M. Lupton, Dirk-Peter Herten and Jan Vogelsang, Differentiation between shallow and deep charge trap states on single poly(3-hexylthiophene) chains through fluorescence photon statistics, ChemPhysChem 16, 3578 (2015),

[8] Hongzhen Lin, Seyed R. Tabaei, Daniel Thomsson, Oleg Mirzov, Per-Olof Larsson and Ivan G. Scheblykin, Fluorescence blinking, exciton dynamics and energy transfer domains in single conjugated polymer chains, J. Am. Chem. Soc. 130, 7042 (2008),

[9] Ji Yu, Dehong Hu and Paul F. Barbara, Unmasking electronic energy transfer of conjugated polymers by suppression of O_2 quenching, Science 289, 1327 (2000),

[10] David A. Vanden Bout, Wai-Tak Yip, Dehong Hu, Dian-Kui Fu, Timothy M. Swager and Paul F. Barbara, Discrete intensity jumps and intramolecular electronic energy transfer in the spectroscopy of single conjugated polymer molecules, Science 277, 1074 (1997),

[11] Jan Vogelsang, Takuji Adachi, Johanna Brazard, David A. Vanden Bout and Paul F. Barbara, Self-assembly of highly ordered conjugated polymer aggregates with long-range energy transfer, Nature Mat. 10, 942 (2011),

[12] Hongzhen Lin, Rafael Camacho, Yuxi Tian, Theo E. Kaiser, Frank Würthner and Ivan G. Scheblykin, Collective fluorescence blinking in linear J-aggregates assisted by long-distance exciton migration, Nano Lett. 10, 620 (2010),

[13] Aboma Merdasa, Angel J. Jimenez, Rafael Camacho, Matthias Meyer, Frank Würthner and Ivan G. Scheblykin, Single Lévy states-disorder induced energy funnels in molecular aggregates, Nano Lett. 14, 6774 (2014),

[14] Andreas Reisch, Pascal Didier, Ludovic Richert, Sule Oncul, Youri Arntz, Yves Mély and Andrey S. Klymchenko, Collective fluorescence switching of counterion-assembled dyes in polymer nanoparticles, Nature Comm. 5:4089 (2014),

[15] Duncan P. Ryan, Peter M. Goodwin, Chris J. Sheehan, Kevin J. Whitcomb, Martin P. Gelfand and Alan Van Orden, Mapping emission from clusters of CdSe/ZnS nanoparticles, J. Phys. Chem. C 122, 4046 (2018),

[16] Douglas P. Shepherd, Kevin J. Whitcomb, Kenneth K. Milligan, Peter M. Goodwin, Martin P. Gelfand and Alan Van Orden, Fluorescence intermittency and energy transfer small clusters of semiconductor quantum dots, J. Phys. Chem. C 114, 14831 (2010),

[17] G. A. Jones and D. S. Bradshaw, Resonance energy transfer : from fundamental theory to recent applications, Front. Phys. 7, 100 (2019),

[18] F. C. de Schryver, T. Vosch, M. Cotlet, M. van der Auweraer, K. Müllen and J. Hofkens, Energy dissipation in multichromophoric single dendrimers, Acc. Chem. Res. 38, 514 (2005),

[19] G. D. Scholes, G. R. Fleming, A. Olaya-Castro and R. van Grondelle, Lessons from nature about solar light harvesting, Nature Chem. 3, 763 (2011),

[20] C. E. Rowland, I. Fedin, H. Zhang, S. K. Gray, A. O. Govorov, D. V. Talapin and R. D. Schaller, Picosecond energy transfer and multiexciton transfer outpaces Auger recombination in binary CdSe nanoplatelet solids, Nature Materials 14, 484 (2015),

[21] S. Ithurria, M. D. Tessier, B. Mahler, R. P. S. M. Lobo, B. Dubertret and Al. L. Efros, Colloidal nanoplatelets with two-dimensional electronic structures, Nature Materials 10, 936 (2011),

[22] Matthew Pelton, Carrier dynamics, optical gain, and lasing with colloidal quantum wells, J. Phys. Chem. C 122, 10659 (2018),

[23] Benjamin T. Diroll, Colloidal quantum wells for optoelectronic devices, J. Mater. Chem. C 8, 10628 (2020),

[24] Jiahao Yu and Rui Chen, Optical properties and applications of two-dimensional CdSe nanoplatelets, InfoMat. 2, 905 (2020),

[25] B. Guzelturk, O. Erdem, M. Olutas, Y. Kelestemur and H. V. Demir, Stacking in colloidal nanoplatelets : tuning excitonic properties, ACS Nano 8, 12524 (2014),

[26] Y. Gao, M. C. Weidman and W. A. Tisdale, CdSe nanoplatelet films with controlled orientation of their transition dipole moment, Nano Lett. 17, 3837 (2017),

[27] B. Guzelturk, M. Olutas, S. Delikanli, Y. Kelestemur, O. Erdem and H. V. Demir, Nonradiative energy transfer in colloidal CdSe nanoplatelet films, nanoscale 7, 2545 (2015),

[28] M. D. Tessier, C. Javaux, I. Maksimovic, V. Loriette and B. Dubertret, Spectroscopy of single CdSe nanoplatelets, ACS Nano 6, 6751 (2012),

[29] F. Feng, L. T. NGuyen, M. Nasilowski, B. Nadal, B. Dubertret, L. Coolen and A. Maître, Consequence of shape elongation on emission asymmetry for colloidal CdSe/CdS nanoplatelets, Nano Research 11, 3593 (2018),

[30] Jiawen Liu, Lilian Guillemeney, Arnaud Choux, Agnès Maître, Benjamin Abécassis and Laurent Coolen, Fourier imaging of single self-assembled CdSe nanoplatelet chains and clusters reveals out-of-plane dipole contribution, ACS Photonics 7, 2825 (2020),

[31] B. Abécassis, M. D. Tessier, P. Davidson and B. Dubertret, Self-assembly of CdSe nanoplatelets into giant micrometer-scale needles emitting polarized light, Nano Lett. 14, 710 (2014),

[32] S. Jana, T. N. T. Phan, C. Bouet, M. D. Tessier, P. Davidson, B. Dubertret and B. Abécassis, Stacking and colloidal stability of CdSe nanoplatelets, Langmuir 31, 10532 (2015),

[33] S. Jana, P. Davidson and B. Abécassis, CdSe nanoplatelets : living polymers, Angew. Chem. Int. Ed. 55, 9371 (2016),

[34] B. Abécassis, Three-dimensional self assembly of semiconducting colloidal nanocrystals : from fundamental forces to collective optical properties, ChemPhysChem 17, 618 (2016),

[35] W. D. Kim, D.-E. Yoon, D. Kim, S. Koh, W. K. Bae, W.-S. Chae and D. C. Lee, Stacking of colloidal CdSe nanoplatelets into twisted ribbon superstructures, J. Phys. Chem C 123, 9445 (2019),

[36] E. M. Y. Lee and W. A. Tisdale, Determination of exciton diffusion length by transient photoluminescence quenching and its application to quantum dot films, J. Phys. Chem. C 119, 9005 (2015),

[37] N. Kholmicheva, P. Moroz, H. Eckard, G. Jensen and M. Zambov, Energy transfer in quantum dot solids, ACS Energy Lett. 2, 154 (2017),

[38] G. M. Akselrod, F. Prins, L. V. Poulikakos, E. M. Y. Lee, M. C. Weidman, A. J. Mork, A. P. Willard, V. Bulovic and W. A. Tisdale, Subdiffusive exciton transport in quantum dot solids, Nano Lett. 14, 3556 (2014),

[39] Jiawen Liu, Lilian Guillemeney, Benjamin Abécassis and Laurent Coolen, Long range energy transfer in self-assembled stacks of semiconducting nanoplatelets, Nano Lett. 20, 3465 (2020),

[40] Lilian Guillemeney, Laurent Lermusiaux, Guillaume Landaburu, Benoît Wagnon and Benjamin Abécassis, Curvature and self-assembly of semi-conducting nanoplatelets, Commun. Chem. 5, 7 (2022),

[41] Christophe Galland, Yagnaseni Ghosh, Andrea Steinbrück, Milan Sykora, Jennifer A. Holligsworth, Victor I. Klimov and Han Htoon, Two types of luminescence blinking revealed by spectroelectrochemistry of single quantum dots, Nature 479, 203 (2011),

[42] Elena V. Shornikova, Dmitri R. Yakovlev, Louis Biadala, Scott A. Crooker, Vasilii V. Belykh, Mikhail V. Kochiev, Alexis Kuntzmann, Michel Nasilowski, Benoît Dubertret and Manfred Bayer, Negatively charged excitons in CdSe nanoplatelets, Nano Lett. 20, 1370 (2020),

[43] Lintao Peng, Matthew Otten, Abhijit Hazarika, Igor Coropceanu, Moritz Cygorek, Gary P. Wiederrecht, Pawel Hawrylak, Dmitri V. Talapin and Xuedan Ma, Bright trion emission from semiconductor nanoplatelets, Phys. Rev. Mat. 4, 056006 (2020),

[44] Lintao Peng, Wooje Cho, Xufeng Zhang, Dmitri Talapin and Xuedan Ma, Observation of biexciton emission from single semiconductor nanoplatelets, Phys. Rev. Mat. 5, L051601 (2021),

[45] Shawn Irgen-Gioro, Yue Wu, Rafael Lopez-Arteaga, Suyog Padgaonkar, Jack N. Olding and Emily A. Weiss, Evidence for two time scale-specific blinking mechanisms in room-temperature single nanoplatelets, J. Phys. Chem. C 125, 13485 (2021),

[46] Stijn O. M. Hinterding, Bastiaan B. V. Salzmann, Sander J. W. Vonk, Daniel Vanmaekelbergh, Bert M. Weckhuysen, Eline M. Hutter and Freddy T. Rabouw, Single trap states in single CdSe nanoplatelets, ACS Nano 15, 7216 (2021),

[47] Xuedan Ma, Benjamin T. Diroll, Wooje Cho, Igor Fedin, Richard D. Schaller, Dmitri V. Talapin, Stephen K. Gray, Gary P. Wiederrecht and David J. Gosztola, Size-Dependent biexciton quantum yields and carrier dynamics of quasi-two-dimensional core/shell nanoplatelets, ACS Nano 11, 9119 (2017),

[48] Barry D. Hughes, Random walks and random environments, Clarendon Press, Oxford (1995),

[49] Qiuyang Li and Tianquan Lian, Area- and thickness-dependent biexciton Auger recombination in colloidal CdSe nanoplatelets: breaking the “universal volume scaling law”, Nano Lett. 17, 3152 (2017),

[50] John P. Philbin, Alexandra Brumberg, Benjamin T. Diroll, Wooje Cho, Dmitri V. Talapin, Richard D. Schaller and Eran Rabani, Area and thickness dependence of Auger recombination in nanoplatelets, J. Chem. Phys. 153, 054104 (2020),

[51] Chunxing She, Igor Fedin, Dmitriy S. Dolzhnikov, Arnaud Demortière, Richard D. Schaller, Matthew Pelton and Dmitri V. Talapin, Low-threshold stimulated emission using colloidal quantum wells, Nano Lett. 14, 2772 (2014),

[52] Elad Benjamin, Venkata Jayasurya Yallapragada, Daniel Amgar, Gaoling Yang, Ron Tenne and Dan Oron, Temperature dependence of excitonic and biexcitonic decay rates in colloidal nanoplatelets by time-gated photon correlation, J. Phys. Chem. Lett. 11, 6513 (2020),

[53] Shuo Dong, Sougata Pal, Jie Lang, Yinthai Chan, Oleg V. Prezhdo and Zhi-Heng Loh, Sub-picosecond Auger-mediated hole-trapping dynamics in colloidal CdSe/CdS core/shell nanoplatelets, ACS Nano 10, 9370 (2016),

[54] S. Wang, C. Querner, T. Dadosh, C. H. Crouch, D. S. Novikov and M. Drndic, Collective fluorescence enhancement in nanoparticle clusters, Nature Comm. 2:364 (2011),

[55] S. Jana, M. de Frutos, P. Davidson and B. Abécassis, Ligand-induced twisting of nanoplatelets and their self-assembly into chiral ribbons, Science Adv. DOI 10.1126/sciadv.1701483.